

Mean Field Control for Efficient Mixing of Energy Loads

David Métivier^{1,*} and Michael Chertkov^{1,2,†}

¹*CNLS & T-4, LANL, Los Alamos, NM*

²*Skoltech, Moscow, Russia*[†]

(Dated: May 4, 2021)

We study an Ensemble of Energy Loads controlled via coordinated, implementation-light, randomized on/off switching. We show that Mean Field Control with nonlinear feedback on the cumulative consumption, assumed available to the aggregator via direct physical measurements of the energy flow, allows the ensemble to recover from its use in the Demand Response significantly faster than in the case of the fixed feedback. When the nonlinearity is sufficiently strong, the total instantaneous energy consumption of the ensemble shows super-relaxation—it stabilizes to the steady state much faster than the underlying probability distribution of the devices over their state space, while also leaving almost no devices outside of the comfort zone.

* metivier@lanl.gov

† chertkov@lanl.gov

I. INTRODUCTION

This manuscript is devoted to analysis of how a large ensemble of energy-consuming loads is seen by a middle-ground, profit-seeking entity coined “aggregator.” The aggregator is set to balance between the following two, generally conflicting, sides: (a) making the ensemble responsive and available for the system operator’s demand response (DR) [25] action, which is aimed to balance, with the least delay possible, all generation and loads originating from resources and customers which cannot be controlled efficiently, and (b) avoiding putting the controlled ensemble-forming customers/loads at risk of spending too much time outside of their comfort zone.

We consider the following basic setting discussed extensively (with some variations) in multiple studies [2, 3, 6, 8, 9, 14, 15, 20, 24]:

- The ensemble is formed by the aggregator from similar loads.
- The air conditioner load in an apartment is considered. When a load does (does not) consume electricity, i.e. when it is switched on (off), the temperature in the apartment decreases (increases).
- By default, i.e., in their normal operational mode, when no signal from the aggregator arrives, the loads function according to the so-called “bang-bang” control—the air conditioner is switched on (off), the temperature reaches x_{\downarrow} (x_{\uparrow}), and then the air conditioner is switched off (on). Here we assume that the outside temperature and the air conditioner capacity are such that a load never reaches a point of dynamic equilibrium thus it is always cycling in its mixed (temperature + on/off) phase space.
- The aggregator controls the ensemble by communicating the same control signal to all loads. The signal overrides the default control.

Already, in the earliest studies on the subject a significant complication of the setting, coined “cold load pick up” [4, 8, 14, 20], was revealed—a period of extensive use of the ensemble in the DR leads to synchronization of load dynamics along the cycle, turning the ensemble from a useful, flexible reserve to an uncontrollable customer whose energy consumption oscillations should be compensated by some other means. Therefore every period of use, when the ensemble is utilized for DR, should follow a grace period, during which the loads are not used for DR, to ensure that the ensemble gets back to an unsynchronized, i.e., well-mixed steady state. The natural stochasticity of the system will eventually lead to the mixing/homogenization of loads within the ensemble. However, the natural mixing is typically weak, so one plausible strategy for the aggregator becomes to relax the default (bang-bang) control policy to achieve a faster mixing (and a shorter grace period) while also keeping the number of loads outside of the comfort zone to a minimum.

As shown in several studies [1, 2, 5, 15, 21], randomization of the control policy [1, 2, 5] and diversification/inhomogeneity of load types within the ensemble [15, 21] both help to accelerate the mixing. In this manuscript we continue to focus on the same task (acceleration); however, we explore a new option related to the so-called Mean-Field Control [12, 13, 19, 23].

This manuscript version of the mean-field control is built on the assumption that the aggregator measures and communicates to the loads the total energy consumption of the ensemble (broadcasting the same signal to all and without delays), and then the loads use a **NONLINEAR** randomization policy depending on the mean-field (meaning averaged over the ensemble) observable.

Significant for massive adaptation of the DR technology, this scheme is **SECURE** and **PRIVATE** because the aggregator does not require access to the consumption of individual loads. The aggregator only needs access to the meter located at the head of the line feeding all the loads—this is under assumptions that the loads are geographically collocated, that they are connected to the same feeder, and that both the consumption of other loads not contributing to the ensemble and also any losses within the feeder are measured/known independently.

II. MAIN RESULTS OF THE MANUSCRIPT

In this manuscript we analyze mixing, i.e., relaxation to a steady state, in a large ensemble of energy loads of the thermostatically controlled load type. We specifically focus on the nonlinear control, where dynamics of an individual device depend on the collective information about the instantaneous consumption of the ensemble—the information which is readily available through physical measurements of the aggregated line flow (if the devices are collocated)—and thus the control does not require receiving any private information from individual devices.

Within the model considered and assuming broadcast (one way) communication from the aggregator to individual devices of their ensemble-common, adjustable switch on/off rate, we continue analysis of previous work [5, 21] and investigate the power of randomization on the overall performance of the ensemble. The new significant emphasis of this manuscript is on the possibility for the Poisson rate, uniform across the ensemble for switching on/off when a device is outside the comfort zone, to be nonlinear and moreover to depend on the independently measured, instantaneous, cumulative (thus the term mean field) consumption of the ensemble. Mixing of the ensemble, i.e., the speed of the ensemble relaxation back to its steady state after a significant perturbation due to ensemble involvement in the DR services, is analyzed. We discover the following:

- The nonlinear stochastic control of the mean-field type results in significant enhancement of the mixing—a decrease of the relaxation time.
- The basic mechanism behind this acceleration is the real-time mean-field adjustment, which stabilizes the total consumed energy. This stabilization can be done without almost any oscillations if the control is tuned correctly and while leaving almost no devices outside of their comfort zone.
- A regime of super-relaxation can be reached, where relevant total consumption decays quickly while other characteristics of the ensemble undergo much slower oscillatory relaxation to the steady state.

Material in the rest of the manuscript is organized as follows. We formulate the problem, set up a properly formalized, stochastic, temporal model, and then transition to a probabilistic Nonlinear Fokker–Planck (NFP) description for the ensemble of devices in Section III. The NFP equations are analyzed theoretically in Section IV, where we first describe the stationary solution in Section IV A, and then in Section IV B we analyze the long-time regime where dynamic corrections to the steady state are sufficiently small to be analyzed perturbatively. We derive a closed-form spectral equation describing the rate of decay and oscillations of the correction to the steady state and analyze different situations in the context of their contribution to the instantaneous consumer energy both analytically and numerically. Section V is devoted to discussion of the direct numerical simulations of a large-but-finite ensemble and their comparison with the aforementioned theoretical predictions. We conclude with a summary and brief discussion of the path forward in Section VI.

III. PROBLEM FORMULATION: FROM STOCHASTIC EQUATIONS TO NONLINEAR FOKKER-PLANCK

In this section we introduce a stochastic, nonlinear model describing dynamics of many energy loads, for example, identical air conditioning units operating in identical apartments, aggregated in an ensemble.

We assume that all devices in the ensemble follow the same set of rules described in terms of the device’s state, $(x(t), \sigma(t))$, where the continuously valued $x(t)$ is the temperature measured inside in the apartment associated with the device (just temperature in the following) and the binary $\sigma(t)$ shows if the device is in

the switch-on, $\sigma(t) = +1$, or switch-off, $\sigma(t) = -1$, mode respectively at the moment of time, t . The state of the device evolves in time, according to the following rules:

$$\forall t: \quad \frac{dx}{dt} = \begin{cases} -v, & \sigma = +1 \\ v, & \sigma = -1, \end{cases} \quad (1)$$

$$\sigma(t+dt) = \begin{cases} \sigma(t), & x(t) \in [x_{\downarrow}; x_{\uparrow}] \\ -\sigma(t), & x(t) < x_{\downarrow} \text{ with probability } r_{\uparrow \rightarrow \downarrow} dt \\ -\sigma(t), & x(t) > x_{\uparrow} \text{ with probability } r_{\downarrow \rightarrow \uparrow} dt \end{cases}, \quad (2)$$

representing a deterministic, limited-range (also called ‘‘bang-bang’’) control implemented automatically and a stochastic/randomized ensemble control implemented in response to the signal broadcasted by the aggregator, respectively. Here in Eq. (1), $\pm v$ describe the instantaneous rate of the temperature, $x(t)$, change at the moment of time t , depending on if the air conditioner is switched on or off and $[x_{\downarrow}; x_{\uparrow}]$ is the preset temperature interval for the automatic control, while $r_{\uparrow \rightarrow \downarrow}$, $r_{\downarrow \rightarrow \uparrow}$ in Eq. (2) are the two distinct rates of the Poisson switching of the device’s mode from on-to-off and off-to-on, respectively, communicated by the aggregator.

In our previous manuscript, [21] the Poisson rates $r_{\uparrow \rightarrow \downarrow}$ and $r_{\downarrow \rightarrow \uparrow}$ were considered equal to each other and moreover constant. The main point of this manuscript is to explore the possibility of controlling the two rates not only independently but also, and most importantly, in a nonlinear way. We consider here the nonlinearity of a special kind—associated with the mean-field control (often referred to in the literature as the mean-field game [12, 13, 19, 23]), where the Poisson rates are dependent on the instantaneous state of the entire ensemble. Specifically, we consider the possibility for the rates to depend on the instantaneous value of the total number of the devices which are switched on. This specific choice is dictated by direct availability of the observable—total number of the devices—through physical observation of the integral (aggregated) energy/power consumption of the geographically collocated ensemble.

To close description of the model, one needs to transition from Eqs. (1, 2), which describe dynamics of the individual device in its phase space, (x, σ) , also illustrated in Fig. (1), to description of the ensemble as the whole, given in terms of its two-component Probability Density Distribution (PDD) vector,

$$P(x|t) \doteq \begin{pmatrix} P_{\uparrow}(x|t) \\ P_{\downarrow}(x|t) \end{pmatrix}. \quad (3)$$

In the asymptotic case of the ensemble consisting of infinitely many devices with the same characteristics (the same $v, x_{\downarrow}, x_{\uparrow}$) and following the same switching protocol (the same $r_{\uparrow \rightarrow \downarrow}$ and $r_{\downarrow \rightarrow \uparrow}$), the PDD vector, $P(x|t)$, is governed by the system of coupled Nonlinear Fokker–Planck (NFP) equations following directly from the model definition given by Eqs. (1, 2). (See also [21] and references therein, for example, to the generic textbooks [10, 11, 27] for discussion of the transition from the individual device/particle level to the collective/ensemble description.)

$$\partial_t P(x|t) = \mathcal{L}P(x|t), \quad (4)$$

$$\mathcal{L}P \doteq \begin{pmatrix} v & 0 \\ 0 & -v \end{pmatrix} \partial_x P - \begin{pmatrix} r_{\uparrow \rightarrow \downarrow} & -r_{\downarrow \rightarrow \uparrow} \\ -r_{\uparrow \rightarrow \downarrow} & r_{\downarrow \rightarrow \uparrow} \end{pmatrix} P. \quad (5)$$

We are seeking a properly normalized solution of Eq. (4):

$$N_{\uparrow}(t) + N_{\downarrow}(t) = 1, \quad N_{\uparrow, \downarrow}(t) \doteq \int dx P_{\uparrow, \downarrow}(x|t), \quad (6)$$

where $N_{\uparrow, \downarrow}(t)$ counts proportions of devices that are switched on and off, respectively.

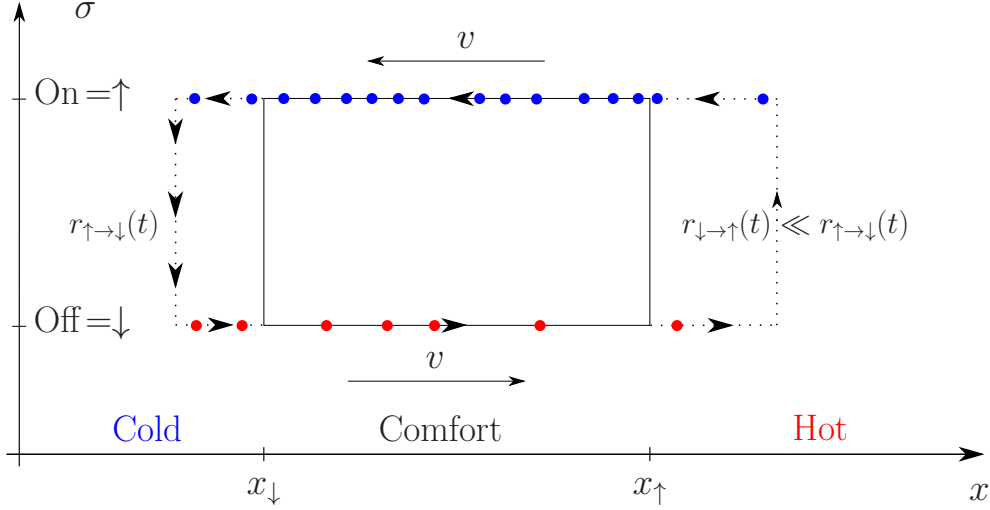


Figure 1. Schematic illustration of an instantaneous device distribution and dynamics in the (x, σ) phase space, where x is the (continuous) temperature and the discrete (two-level) designation $\sigma = \pm$ marks whether the device (air conditioner) is switched on, $\sigma = +1$, or off, $\sigma = -1$. Instantaneous placement of cold (blue) and hot (red) loads at some t illustrates an inhomogeneous case where a majority of the devices are on. In this case MF control makes the transition rate from off-to-on, $r_{\uparrow \rightarrow \downarrow}$, higher than the on-to-off rate, $r_{\downarrow \rightarrow \uparrow}$, thus boosting equalization of the two densities (in comparison with the case where the two rates are equal).

The study of [21] has focused on analysis of the case with Poisson rates that are constant and equal to each other in Eq. (5), i.e., $r_{\downarrow \rightarrow \uparrow} = r_{\uparrow \rightarrow \downarrow}$. In this manuscript we analyze the case when the Poisson rates do depend on $P(x|t)$ explicitly, thus making the FP equation (4) nonlinear. The nonlinearity we study represents a control which is both available to the aggregator and also sensible in terms of improving the speed of the system relation as seen by the system operator. One naturally asks: what type of the nonlinear feedback is sensible? A natural suggestion of a plausible answer to the question comes from the already stressed fact that the total instantaneous consumption of the geographically collocated ensemble may be readily available through direct physical measurements, and moreover this is the only object for which relaxation/mixing is of a significance for the aggregator. Therefore, we naturally consider the nonlinear feedback on the instantaneous aggregated consumption, N_{\uparrow} :

$$r_{\uparrow \rightarrow \downarrow}(N_{\uparrow}(t), x) = \begin{cases} g(N_{\uparrow}(t)), & x < x_{\downarrow} \\ 0 & \text{otherwise} \end{cases}, \quad (7)$$

$$r_{\downarrow \rightarrow \uparrow}(N_{\uparrow}(t), x) = \begin{cases} g(N_{\downarrow}(t)) = g(1 - N_{\uparrow}(t)), & x > x_{\uparrow} \\ 0 & \text{otherwise} \end{cases}. \quad (8)$$

where the freedom over the choice of $g(N)$ expresses the functional dependencies we will experiment with in the following.

Notice the similarity of the nonlinearity in the Poisson rate with the mean-field coupling analyzed in plasma physics [18, 22, 28] and synchronizing networks [16, 17, 26], where the nonlinearity is associated with the names of Vlasov and Kuramoto, respectively. The Vlasov equation [18, 22, 28] is used in plasma physics to describe long-range interactions in the situation where electrons contribute collectively through the mean electric field while collisions between particles (thus, many-body interactions) are neglected. The

Kuramoto system [16, 17, 26] models spontaneous collective synchronization of oscillators coupled all-to-all nonlinearly with equal strength. The dynamics of the Kuramoto system are the result of a competition between mixing due to inhomogeneities (over natural frequencies) and synchronizing effect of the mean-field coupling.

To get a simple intuition on the benefit of having non-constant and nonlinear Poisson rates already at this stage, let us consider $g(N) = N/q$, where $q = 1/2$ is the equilibrium value of N_\uparrow and N_\downarrow . If, due to a perturbation, there appears to be more devices in the “on” state, $N_\uparrow(t) > q$, then the probability of them switching off will be larger,

$$r_{\uparrow \rightarrow \downarrow} = \frac{N_\uparrow}{q} > 1 > \frac{1 - N_\uparrow}{q} = r_{\downarrow \rightarrow \uparrow},$$

so that N_\uparrow will decrease, and vice versa. Therefore, one anticipates that this simple feedback mechanism will accelerate the desired relaxation, $N_\uparrow(t) \rightarrow q$.

In the next section we focus on theoretical analysis of the NFP Eqs. (4).

IV. ANALYSIS OF THE NONLINEAR FOKKER-PLANCK EQUATION

A. Stationary Solution

Let us first look at a stationary, i.e., time-independent, solution of the NFP system of Eqs. (4,5,7,8), which in this case reduces to

$$0 = \begin{cases} \begin{pmatrix} v & 0 \\ 0 & -v \end{pmatrix} \partial_x P^{(\text{st})} + \begin{pmatrix} -1 & 0 \\ 1 & 0 \end{pmatrix} r_\uparrow P^{(\text{st})}, & x < x_\downarrow \\ \begin{pmatrix} v & 0 \\ 0 & -v \end{pmatrix} \partial_x P^{(\text{st})}, & x_\downarrow < x < x_\uparrow \\ \begin{pmatrix} v & 0 \\ 0 & -v \end{pmatrix} \partial_x P^{(\text{st})} + \begin{pmatrix} 0 & 1 \\ 0 & -1 \end{pmatrix} r_\downarrow P^{(\text{st})}, & x > x_\uparrow \end{cases}, \quad (9a)$$

$$r_\uparrow \doteq g(q_\uparrow), \quad r_\downarrow \doteq g(q_\downarrow), \quad (9b)$$

$$q_\uparrow \doteq \int P_\uparrow^{(\text{st})}(x') dx', \quad q_\downarrow \doteq \int P_\downarrow^{(\text{st})}(x') dx', \quad q_\uparrow + q_\downarrow = 1. \quad (9c)$$

Here q_\uparrow and q_\downarrow are time-independent constants, which should be self-consistently defined. Given the fixed values of the two constants, Eqs. (9) are actually linear and, moreover, easy to solve (see, for example,

Ref. [21]), resulting in

$$P^{(\text{st})}(x) = \frac{1}{N^{(\text{st})}} \begin{pmatrix} 1 \\ 1 \end{pmatrix} \begin{cases} e^{\frac{r_{\uparrow}(x-x_{\downarrow})}{v}}, & x < x_{\downarrow} \\ 1 & , x_{\downarrow} < x < x_{\uparrow} \\ e^{\frac{r_{\downarrow}(x_{\uparrow}-x)}{v}}, & x > x_{\uparrow} \end{cases} , \quad (10)$$

$$N^{(\text{st})} \doteq 4 \left(\frac{v}{r} + \frac{x_{\uparrow} - x_{\downarrow}}{2} \right). \quad (11)$$

Enforcing the self-consistency condition (9c), one arrives at the conclusion that the total probability of devices to be in the cold and hot states are constant and equal to each other (and thus independent of r_{\pm}): $q_{\uparrow} = q_{\downarrow} = \frac{1}{2}$. Then the steady state Poisson rates are also equal to each other: $r \doteq g(1/2)$.

The fraction of devices residing at the moment of time, t , outside the comfort zone,

$$N_{\text{out}}(t) = \int_{x > x_{\uparrow} \text{ or } x < x_{\downarrow}} (P_{\uparrow}(x, t) + P_{\downarrow}(x, t)) dx, \quad (12)$$

reduces to the following compact formula when considered in the steady state regime:

$$N_{\text{out}}^{(\text{st})} = \frac{1}{1 + r\tau/4}. \quad (13)$$

where $\tau \doteq 2(x_{\uparrow} - x_{\downarrow})/v$ is the cycling period in the case of the instantaneous bang-bang switching ($r \rightarrow \infty$ limit).

Notice the emergence of the following two opposite asymptotic regimes: $N_{\text{out}}^{(\text{st})} \rightarrow 0$ at $r\tau \rightarrow \infty$ and $N_{\text{out}}^{(\text{st})} \rightarrow 1$ at $r\tau \rightarrow 0$. In practice, we would like $N_{\text{out}}^{(\text{st})}$, measuring the level of devices/customers discomfort, to be as small as possible. On the other hand, choosing a large $r_{\uparrow, \downarrow}$ is not desirable as it results in a weak control of mixing—this remains the main target of our analysis. Therefore, we are actually interested in exploring a middle ground, thus developing controls with a good tradeoff between efficient mixing and customer comfort.

Testing the efficiency of mixing requires non-stationary analysis of the NFP system of equations, which we shift our attention to in the remainder of this section. We aim to show that proper choice of the MF nonlinearity will result in a good tradeoff between the speed of mixing and the level of customer's comfort.

B. Dynamic Linearization about the Stationary Solution

We are interested in the dynamics resulting in a relaxation to the stationary solution described in the preceding subsection. At the latest stages of the relaxation dynamic, correction to the stationary solution is

small and thus governed by the following linearized equations for the PDD vector:

$$P(x|t) = P^{(st)}(x) + \rho(x, t) \quad , \|\rho\| \ll P^{(st)}, \quad \rho(x|t) \doteq \begin{pmatrix} \rho_{\uparrow}(x|t) \\ \rho_{\downarrow}(x|t) \end{pmatrix}, \quad (14)$$

$$\frac{\partial \rho}{\partial t} - \mathcal{L} \rho = rs \begin{pmatrix} -\chi_{\uparrow} \theta(x < x_{\downarrow}) & \chi_{\downarrow} \theta(x > x_{\uparrow}) \\ \chi_{\uparrow} \theta(x < x_{\downarrow}) & -\chi_{\downarrow} \theta(x > x_{\uparrow}) \end{pmatrix} P^{(st)}(x) + O(\|\rho\|^2), \quad (15)$$

$$\mathcal{L} \doteq \begin{pmatrix} v & 0 \\ 0 & -v \end{pmatrix} \partial_x + r \begin{pmatrix} -\theta(x < x_{\downarrow}) & \theta(x > x_{\uparrow}) \\ \theta(x < x_{\downarrow}) & -\theta(x > x_{\uparrow}) \end{pmatrix}, \quad (16)$$

$$\chi(t) \doteq \begin{pmatrix} \chi_{\uparrow}(t) \\ \chi_{\downarrow}(t) = -\chi_{\uparrow}(t) \end{pmatrix} \doteq \int \rho(x', t) dx', \quad s \doteq \left. \frac{d \log(g(N))}{dN} \right|_{N=1/2}, \quad (17)$$

where $\theta(a)$ is unity if a is true, and it is zero otherwise. Notice that when the right-hand side of Eq. (15) is replaced by zero, the resulting equation becomes the basic (linear) Fokker–Planck equation for which solutions were analyzed in previous work [21]. Looking for the solution of Eq. (15) in the form of a spectral expansion,

$$\rho(x|t) = \sum_{\lambda} \exp(-\lambda t) \rho_{\lambda}(x), \quad (18)$$

one arrives at

$$-(\lambda + \mathcal{L}) \rho_{\lambda} = rs \begin{pmatrix} -\chi_{\lambda; \uparrow} \theta(x < x_{\downarrow}) & \chi_{\lambda; \downarrow} \theta(x > x_{\uparrow}) \\ \chi_{\lambda; \uparrow} \theta(x < x_{\downarrow}) & -\chi_{\lambda; \downarrow} \theta(x > x_{\uparrow}) \end{pmatrix} P^{(st)}(x), \quad (19)$$

where $\chi(t) = \sum_{\lambda} \exp(-\lambda t) \chi_{\lambda}$. Considering χ_{λ} as a vector of fixed constants (which should be found later on from a consistency condition), one can view the right hand side of Eq. (19) as fixed/known too. Then looking for the solution of the inhomogeneous linear differential, Eq. (19), in the form of a sum of an arbitrary zero mode of the operator, $\lambda + \mathcal{L}$, and a particular inhomogeneous solution, one derives

$$\rho_{\lambda}(x) = \begin{cases} c_L e^{\frac{x(r-\lambda)}{v}} \begin{pmatrix} 1 \\ \frac{r}{r-2\lambda} \end{pmatrix}, & x < x_{\downarrow} \\ \begin{pmatrix} c_{c_{\uparrow}} e^{-\frac{\lambda x}{v}} \\ c_{c_{\downarrow}} e^{\frac{\lambda x}{v}} \end{pmatrix}, & x_{\downarrow} < x < x_{\uparrow} \\ c_R e^{-\frac{(r-\lambda)x}{v}} \begin{pmatrix} \frac{r}{r-2\lambda} \\ 1 \end{pmatrix}, & x > x_{\uparrow} \end{cases} + rs \frac{\chi_{\lambda; \uparrow}}{N_Q} \begin{cases} \begin{pmatrix} \frac{e^{\frac{r(x-x_{\downarrow})}{v}}}{\lambda} \begin{pmatrix} 1 \\ \frac{r+\lambda}{r-\lambda} \end{pmatrix} \\ 0 \\ 0 \end{pmatrix}, & x < x_{\downarrow} \\ \begin{pmatrix} 0 \\ 0 \end{pmatrix}, & x_{\downarrow} < x < x_{\uparrow} \\ \begin{pmatrix} -\frac{e^{-\frac{r(x-x_{\uparrow})}{v}}}{\lambda} \begin{pmatrix} \frac{r+\lambda}{r-\lambda} \\ 1 \end{pmatrix} \end{pmatrix}, & x > x_{\uparrow} \end{cases}, \quad (20)$$

where the vector of coefficients, $C = (c_L, c_{c_{\uparrow}}, c_{c_{\downarrow}}, c_R)$, is yet to be fixed by the conditions of the $\rho_{\lambda}(x)$ continuity at $x = x_{\downarrow}$ and $x = x_{\uparrow}$ and an additional self-consistency condition.

Imposing the set of continuity and self-consistency conditions one arrives at the following two families of equations:

$$\frac{re^{\frac{\lambda \tau}{2}}}{r-2\lambda} \left(\frac{4sr^2}{(r-\lambda)(2sr+(r-\lambda)(r\tau+4))} - 1 \right) = 1, \quad (21)$$

$$\frac{re^{\frac{\lambda \tau}{2}}}{r-2\lambda} = 1, \quad (22)$$

where the self-consistency condition, used to derive Eq. (21), was $\chi_{\lambda;\uparrow} = \int dx \rho_{\lambda;\uparrow}(x)$ and Eq. (22) followed from the degenerate version of the continuity condition for the eigenvectors with $\chi_{\lambda;\uparrow} = 0$. In the following we denote the discrete spectrum, emerging from solving Eq. (21) and Eq. (22) as “-”-branch $k \in \mathbb{Z} : \lambda_{k;-}$ and “+”-branch $k \in \mathbb{Z}^* : \lambda_{k;+}$, respectively. A number of remarks are in order. First, let us stress that the two branches—represented by solutions of Eq. (21) and Eq. (22)—coexist, i.e., both branches are included in the sum over λ in the spectral expansion (18). Second, notice that the “+”-branch, described by $\lambda_{k;+}$, (a) is mean-field nonlinearity-independent, and (b) does not contribute to N_{\uparrow} —our main object of interest. Third, the dependence of both branches on x_{\pm} and v is implicit via τ . Fourth, all solutions of Eqs. (21, 22) result in non-negative $\lambda_{k;\pm}$, where $\lambda_{0,+} = 0$ is excluded from the perturbation series because it corresponds to the stationary state described in Section IV A. Finally, fifth, at $s = 0$ one recovers in Eq. (21) the negative solution branch of the bare spectral problem (without the mean-field control) discussed in [21]. In this case, solutions of Eqs. (21,22) are given by

$$k \in \mathbb{Z} : \lambda_{k;\pm}^{(s=0)} = 2\tau^{-1} (\beta - W_k(\pm\beta e^{\beta})). \quad (23)$$

In the following we will denote explicitly the dependency over the mean-field parameter, s , for the “-”-branch as $\lambda_{k;-}^{(s)}$ and omit it in the “+”-branch which is not modified by the mean field. Moreover, as for the $s = 0$ case, we will denote the leading eigenvalue (having the smallest real part) of the “-”-branch by $k = 0$ (and $k = -1$, its complex conjugate, when it becomes complex $\text{Im}(\lambda_{0;-}^{(s=0)}) \neq 0$). Similarly $\lambda_{\pm 1;+}$, which are always complex, will be the two leading eigenvalues of the “+”-branch. All larger $|k| > 1$ will index eigenvalues with larger real part.

1. Asymptotic Analysis of the “-”-branch

One finds through perturbative analysis that in the regime of $r\tau \gg 1$ the eigenvalue of the negative branch with the lowest real part becomes

$$\lambda_{0;-}^{(s)} = \lambda_{0;-}^{(s=0)} + \frac{8s}{r\tau^2} + O\left(\frac{1}{\tau^3 r^2}\right). \quad (24)$$

Note that at $s > 0$, the correction (to the bare solution) is always real and positive, thus leading to a monotonic increase of the relaxation rate, $\text{Re}(\lambda_{k;-}^{(s)})$, with an increase in the (level of) nonlinearity while also keeping the oscillatory contribution, $\text{Im}(\lambda_{k;-}^{(s)})$, intact (in the leading order). The effect is clearly seen in Figs. 2 and 3 representing numerical solution of Eqs. (21, 22).

Another interesting regime is the regime of a weak nonlinearity corresponding to $s \ll 1$ and fixed r . Here the mean-field correction to the spectrum takes the following form:

$$k \in \mathbb{Z} : \lambda_{k;-}^{(s)} = \lambda_{k;-}^{(s=0)} + s\lambda_{k;\epsilon} + O(s^2), \quad \lambda_{k;\epsilon} \doteq \frac{8r^2(r - 2\lambda_{k;-}^{(s=0)})}{(r - \lambda_{k;-}^{(s=0)})^2(r\tau + 4)((r - 2\lambda_{k;-}^{(s=0)})\tau + 4)}. \quad (25)$$

One observes that at sufficiently small r and $s > 0$, $\text{Re}(\lambda_{k;\epsilon})$ is negative; however, it grows with r to become positive at some critical value, which then leads to acceleration of the relaxation as seen on Fig. 3.

2. Effect of the Mean-Field Interaction (Nonlinearity) Shape

The remaining analysis of the spectrum from Eq. (21) is computational, and it is focused on testing the effect of the mean-field nonlinearity. We choose to experiment with r and other parameters in the algebraic

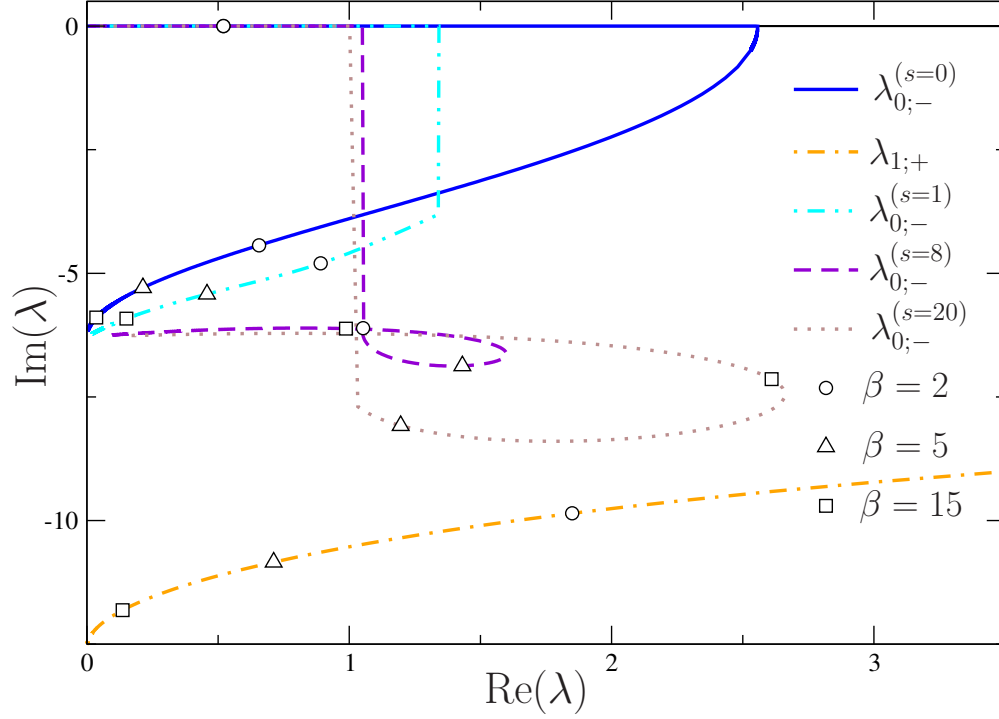


Figure 2. Solution of the spectrum for Eq. (21) in the lower-half plane (picture in the upper-half plane is symmetric) compared for different s where $g(N) = r(2N)^{s/2}$, which is consistent with the definition of s in Eq. (17), which is also shown. The leading eigenvalue of Eq. (22), $\lambda_{1,+}$, is also shown. Curves of different colors correspond to the leading eigenvalues in the bare non-mean-field case (blue) and then to different values of s . Moving along a curve corresponds to changing $r = g(1/2)$ when $\tau = 1$. Dashed vertical lines correspond to the point of discontinuous transition from the regime where the relaxation is of the strict decay type (eigenvalue is real) to the regime where it is of the decay + oscillations type (eigenvalue is complex). (We remind that $\beta = r\tau/4$.)

functional form, $g(N) = r(2N)^{s/2}$, consistent with the definition of s in Eq. (17), while keeping the main characteristic of the ensemble, τ , fixed. The results of the experiments are shown in Figs. (2, 3, 4). Our choice of the functional form is such that the stationary point achieved at different s is the same, characterized by $g(1/2) = r$. We will also initiate dynamics with the same initial condition for $P(x|0)$. This setting allows us a fair quantitative comparison of the effect, measured by s , of the mean-field nonlinearity strength on the transient to the steady state.

V. DIRECT NUMERICAL SIMULATIONS OF THE ENSEMBLE

In this section we complement analytic analysis of our mean-field control model with direct numerical simulation analysis. We experiment with the ensemble of $N = 2 \cdot 10^6$ identical devices following Eqs. (1, 2). In all our experiments the extreme initial condition was chosen where all devices are at the same point of the phase space, $x = x_{\downarrow}$, and $\sigma = +1$, i.e., the devices are on. This initial condition represents the worst case for mixing. The results of the experiments are illustrated in Figs. (5, 6, 7). These experiments, combined

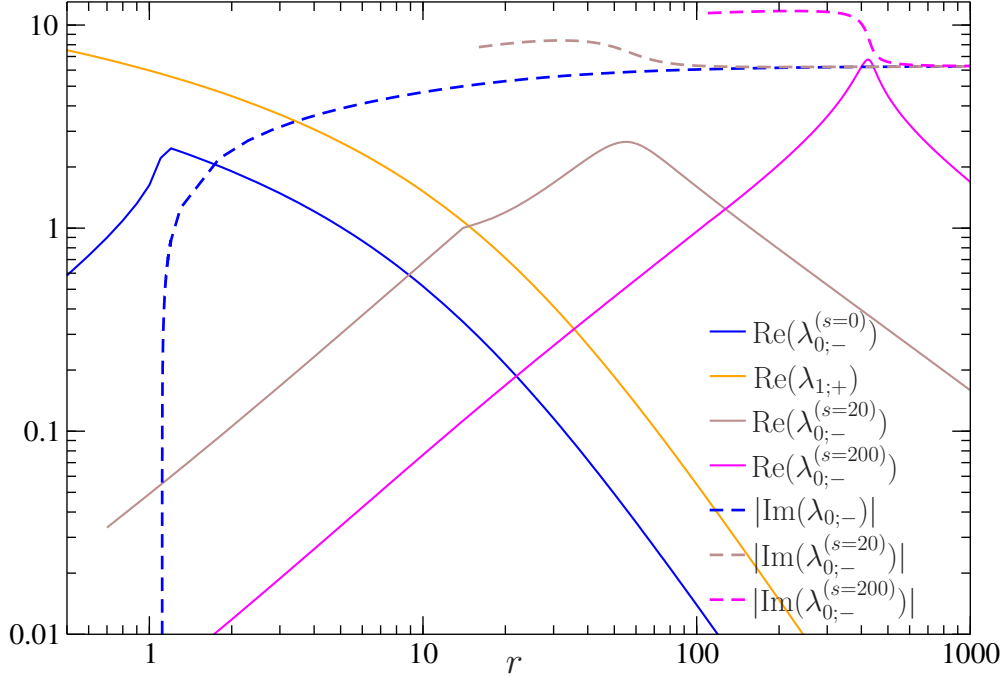


Figure 3. Real (solid line) and imaginary (dashed line) parts for solutions of the spectrum Eqs. (21, 22) evaluated for three values of the mean-field strength ($s = 0, 20, 200$) and shown as a function of r at $\tau = 1$. When, with r increase, the real part of the mean-field eigenvalue crosses the $\text{Re}(\lambda_{0;-}^{(s=0)})$ curve (marked blue), it signals a transition to the regime where the mean-field control results in a faster relaxation to the stationary value. When r is increased further, the mean-field eigenvalue can cross the $\text{Re}(\lambda_{1;+})$ line, which is an indicator that $N_{\uparrow}(t)$ relaxes faster than any other expectations over $P(x|t)$ (super-relaxation). The end of the dashed curves (at sufficiently small r and $s > 0$) corresponds to the discontinuous transition from the relaxation + oscillation regime (at larger r) to the pure relaxation regime (at smaller r). The transition is continuous at $s = 0$. We show the transition to oscillatory relaxation (when $\text{Im}(\lambda) \neq 0$) for the different cases, which is continuous for $s = 0$ and discontinuous otherwise.

with the analytic analysis, have allowed us to uncover the following interesting features of the model.

- **Transition from Pure Relaxation to Relaxation with Oscillations.** In the nonlinear case, $s \neq 0$, there is a transition for the smallest eigenvalue that goes abruptly from real to a pair of the complex conjugated solutions at $\beta = r\tau/4 > \beta_c(\alpha)$. As illustrated above in Fig. 4, the transition is discontinuous—contrary to the case without mean-field control. Fig. 5 tests this transition through direct simulations of the ensemble. We observe that when the leading eigenvalue is still real, e.g., at $\beta = 1$, the dynamics are purely oscillatory, while at the higher values of β , for example, at $\beta = 2$, the relaxation gets an additional oscillatory component. We also find a good agreement between asymptotic and numerical values for the decay rate.
- **Significant Enhancement of the Relaxation by Mean-Field Control.** At a sufficiently large level of nonlinearity, corresponding to small β values, one observes a significant advantage of the mean-field control—an “ear” seen in Fig. 2 at $s > 0$. Specifically, one finds that at the fixed value of nonlinearity, s , one reaches the maximum value of $\text{Re}(\lambda)$ by adjusting r . The maximum increases with the strength of the nonlinearity. For example, at $s = 8$ the maximal value (right tip of the ear) is reached at $\beta \simeq 7$

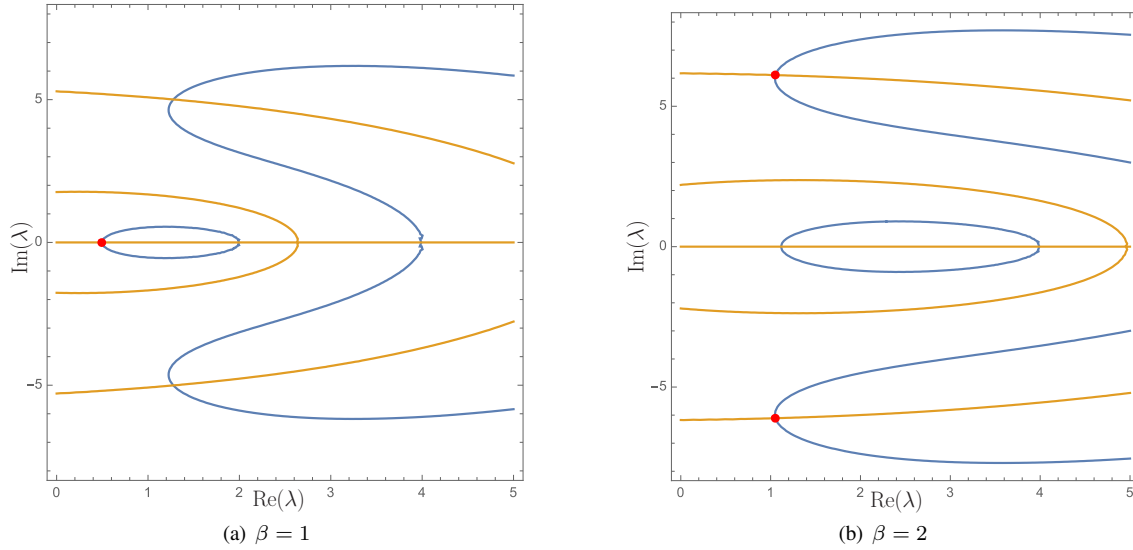


Figure 4. An illustration of solutions of Eq. (21) in the $(\text{Re}(\lambda), \text{Im}(\lambda))$ plane showing zero iso-lines of real (blue) and imaginary (yellow) components of the equation. Any crossing of blue and yellow corresponds to an eigenvalue. Red dots show eigenvalues with the smallest real part. The two sub-figures correspond to two values of β characterizing the purely relaxational and relaxation with oscillations regimes, respectively. Here $s = 8$, and the choice of other parameters is the same as in Fig. (2).

and $\lambda_{0;-}^{(s=8)} = 1.6 \pm 6.6i$, while for the same parameter value (hence the same initial and final state) one gets in the $s = 0$ case without the mean-field control $\lambda_{0;-}^{(s=0)} = 0.13 \pm 5.5i$ (see Fig. 6 for numerical test). This gives the $\simeq 12$ -fold gain in the exponential rate of decay!

- **Sensitivity to the Initial Condition in the Nonlinear Regime.** Dependence of the speed of relaxation on the model parameters, which is illustrated in Fig. 2 and is following from the asymptotic analysis of Section IV B, shows an opportunity for significant enhancement of the relaxation rate for the aggregated ensemble consumption. Extension of the analytic analysis beyond the weakly nonlinear regime does not seem feasible at this stage, and we thus need to rely on numerical experimentation with a finite-sized ensemble to test the case of the strongly nonlinear mean-field control. This analysis (already discussed, in part, above) has confirmed that acceleration of the relaxation speed by the nonlinearity is substantial (see e.g. Fig. (6)), however it has also revealed a significant sensitivity of the relaxation rate on the ensemble Initial Condition (IC). In particular, and as illustrated in Fig. (7), if the IC is concentrated (case 1) in a part of the phase space and the nonlinearity is sufficiently strong, the the PDD vector remains concentrated and does not mix for a long while. This concentration effect disappears when one broadens IC, as shown in the case 2 in Fig. (7). We conclude that to avoid the “trapping” effect, one simply needs to make sure that the ensemble would always (even when used for DR) remain sufficiently widespread over the phase space.
- **Super-Relaxation of the Aggregate Consumption.** The last, but not the least, feature of the model is that the mean-field control is sufficiently large that the aggregate consumption of the ensemble relaxes to its steady value much faster than the entire distribution. This important observation is illustrated in

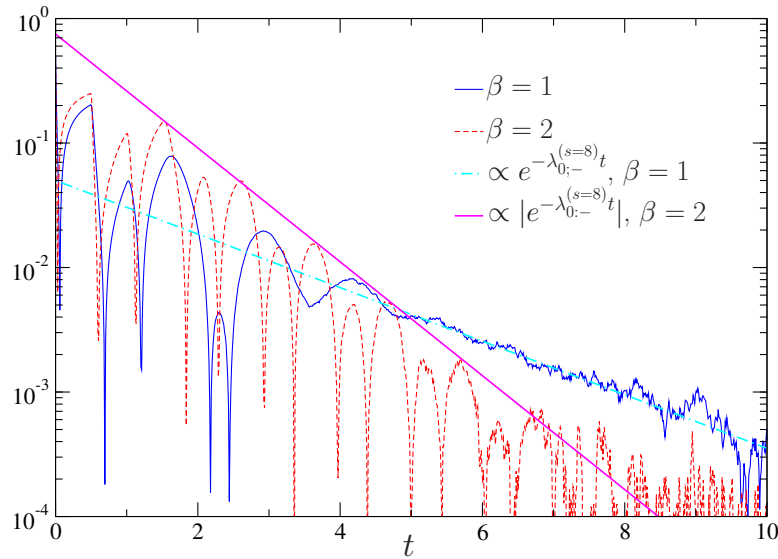


Figure 5. Temporal evolution of $|N_{\uparrow}(t) - 1/2|$, $\beta = 1$, and $\beta = 2$ with $\tau = 1$ and $-x_{\downarrow} = x_{\uparrow} = 1$. The initial condition is the least spread, at $t = 0$. All devices are set to on at $x = x_{\downarrow}$. The corresponding linear decay rates predicted by the dispersion relation Eq. (21) ($\lambda_{0;-}^{(s=8)} = 0.50$ for $\beta = 1$ and $\lambda_{0;-}^{(s=8)} = 1.1 \pm 6.1i$ for $\beta = 2$) shows a good agreement with the numerics, thus confirming transition from the pure relaxation at $\beta = 1$ to the relaxation with oscillations at $\beta = 2$.

Fig. (8). We choose to compare relaxation of $N_{\uparrow}(t)$, corresponding to the total energy consumed by the ensemble, with the following object

$$H_1(t) = A \int \left(|P_1(x|t) - P_1^{(st)}(x)| + |P_2(x|t) - P_2^{(st)}(x)| \right) dx, \quad (26)$$

which accounts for all of the “ \pm ”-modes, contrary to $N_{\uparrow}(t)$, and is dependent only on the “ $-$ ”-branch of the spectrum Eq. (21). (Coefficient A in Eq. (26) is introduced for re-scaling. See caption in Fig. (8) for clarifications.) It is clearly seen in Fig. (8) that the total/aggregate energy consumption of the ensemble, N_{\uparrow} , relaxes to a constant very quickly—much before $H_1(t)$. We emphasize that this important observation is fully consistent with the results of our theoretical analysis in Section IV B, stating that at sufficiently large s (measuring the level of nonlinearity), the leading eigenvalue real part, $\text{Re}(\lambda_{0;-}^{(s)})$, which controls $N_{\uparrow}(t)$ relaxation, is larger than $\text{Re}(\lambda_{1;+})$, controlling relaxation of any other expectations of a general position over $P(x|t)$, including $H_1(t)$ (see also Fig. 3).

VI. CONCLUSION

The main message of this manuscript is in an unexpectedly strong positive effect of the mean-field nonlinear control on mixing in the ensemble of energy loads. Our analytic and computational analyses show that making the transition rates between switch-on and switch-off states to depend on the instantaneous number of devices in the two states accelerates mixing in the ensemble significantly, in comparison

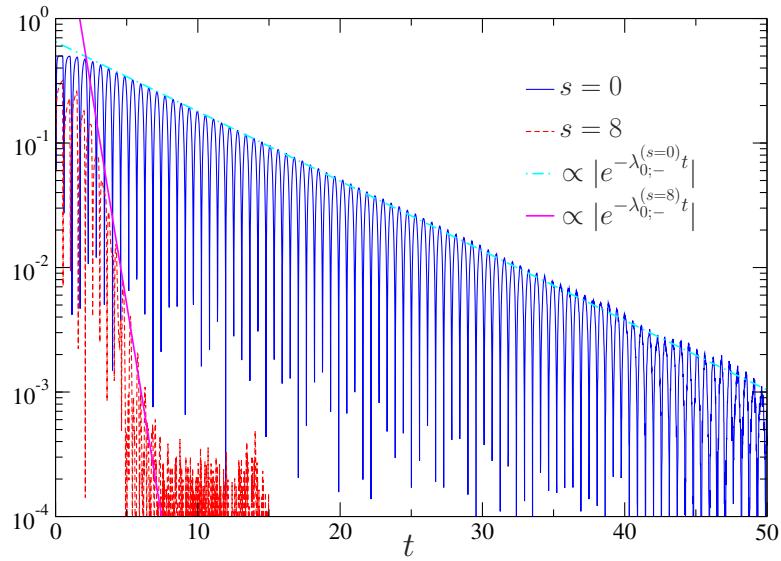


Figure 6. Temporal evolution of $|N_{\uparrow}(t) - 1/2|$ in the simulations where $s = 0$ (no mean-field control) and $s = 8$, $\tau = 1$, $\beta = 7$ and $-x_{\downarrow} = x_{\uparrow} = 1$ for the case with the mean-field control. The initial condition is the least spread—at $t = 0$ all devices are set to on at $x = x_{\downarrow}$. Theoretical predictions that resulted in Eq. (21) show a good agreement with the numerics, where $\lambda_{0;-}^{(s=0)} = 0.13 \pm 5.5i$ and $\lambda_{0;-}^{(s=8)} = 1.6 \pm 6.6i$.

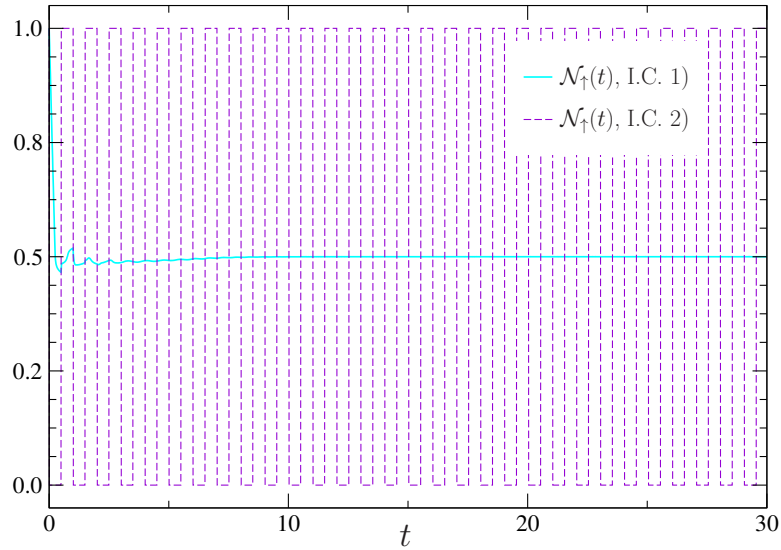


Figure 7. Temporal evolution of $N_{\uparrow}(t)$ in the simulations where $s = 200$, $r = 100$, $\tau = 1$, $-x_{\downarrow} = x_{\uparrow} = 1$. $N = 2 \cdot 10^6$, and the following three IC conditions are shown: (1) uniform over the range $x \in [x_{\downarrow}; x_{\uparrow}]$ and the devices are set to on (least concentrated of the two); (2) a δ -function at $x = x_{\downarrow}$ and all the devices are set to on (most peaked, least spread).

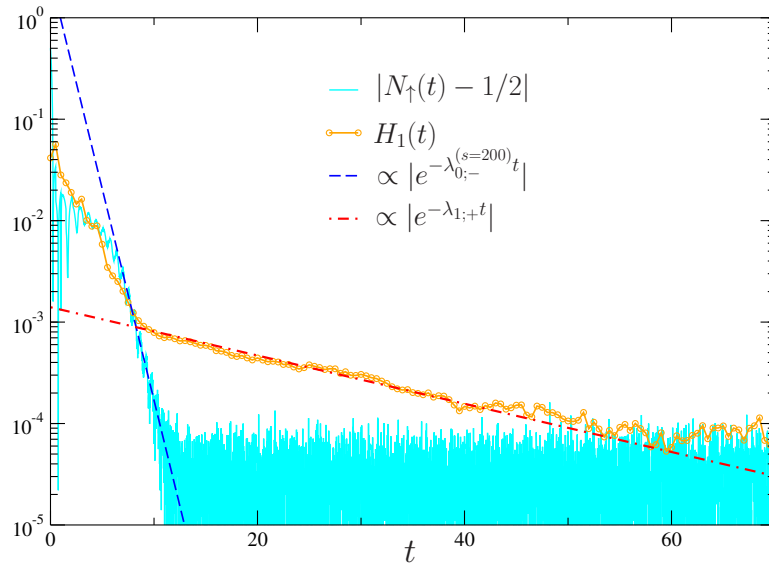


Figure 8. We compare relaxation of $|N_{\uparrow}(t) - 1/2|$ and $H_1(t)$, defined in Eq. (26), for the case 1 of IC from Fig. 7. We observe, consistent with the theoretical analysis of Section IV B, that $N_{\uparrow}(t)$ decays to its equilibrium value with an exponential rate, $\lambda_{0;-}^{(s=200)} = 0.93$, while $H_1(t)$ decay is much slower with $\lambda_{1;+} = 0.055 - 12i$ (super-relaxation). We adjust coefficient A in Eq. (26) to make fluctuations associated with the finite size of the ensemble (seen in the noise observed at large t) comparable for $|N_{\uparrow}(t) - 1/2|$ and $H_1(t)$.

with the bare case of the constant rates. The effect is especially well pronounced at a sufficiently strong level of the mean-field nonlinearity when the relaxation of the probability density distribution vector is almost of the pure decay (no oscillations) type. In this regime we also observe and explain the super-relaxation effect: the total number of the switch-on devices (which is also instantaneous energy consumption of the system) decays to its steady state much faster than any other mode of the probability density distribution vector. We also observe and characterize transitions between pure decay and decay + oscillations regimes.

In the future, we plan to continue further these explorations in the following directions:

- We believe that the majority of features of the ensemble highlighted in the preceding paragraph are universal and robust to modification of the basic model of the device dynamic considered in the manuscript. To verify the universality, we intend to consider a more general model, e.g., what was called the soft model in [5], accounting for dependence of the rate of the temperature change on the temperature itself, $v(x)$.
- It will also be important to investigate the joint effect of the two complementary strategies of the ensemble mixing enhancement: the mean-field control studied in this manuscript and control by randomization discussed in our preceding manuscript [7].
- Analyzing the effectiveness of the mean-field approach for a broader control objective (broader than just mixing enhancement) constitutes another research line to explore. In particular, it will be of interest to consider mean-field generalization of the Markov Decision Process model of the energy load ensemble discussed in [7].

We conclude by noticing, somehow rhetorically, that the phenomenon of mixing enhancement by mean

field—motivated and discussed in this manuscript in the context of the energy system ensemble—may also apply to a much broader class of natural and engineered systems consisting of a large number of similar units or agents, such as particles following a turbulent flow, birds in a flock formation, or robots exploring a landscape.

VII. ACKNOWLEDGEMENTS

The authors acknowledge useful discussions with Marc Vuffray. The work at LANL was carried out under the auspices of the National Nuclear Security Administration of the U.S. Department of Energy under Contract No. DE-AC52-06NA25396. The work was partially supported by DOE/OE/GMLC and LANL/LDRD/CNLS projects.

-
- [1] D. Angeli and P. A. Kountouriotis. A stochastic approach to dynamic-demand refrigerator control. IEEE Transactions on Control Systems Technology, 20(3):581–592, May 2012.
 - [2] A. Bušić and S. Meyn. Distributed Randomized Control for Demand Dispatch. [arxiv:1603.05966](https://arxiv.org/abs/1603.05966), March 2016.
 - [3] A. Bušić and S. Meyn. Ordinary Differential Equation Methods For Markov Decision Processes and Application to Kullback-Leibler Control Cost. [arxiv:1605.04591](https://arxiv.org/abs/1605.04591), May 2016.
 - [4] D.S. Callaway and I.A. Hiskens. Achieving controllability of electric loads. Proceedings of the IEEE, 99(1):184–199, Jan 2011.
 - [5] M. Chertkov and V. Chernyak. Ensemble of thermostatically controlled loads: Statistical physics approach. Scientific Reports, 7, 2017.
 - [6] M. Chertkov, V. Chernyak, and D. Deka. Ensemble control of cycling energy loads: Markov decision approach. In S. Glavaski I. Hiskens J. Stoustrup S. Meyn, T. Samad, editor, Energy Markets and Responsive Grids: Modeling, Control and Optimization. Springer, Series: Institute of Mathematics and Applications, 2018.
 - [7] M. Chertkov, V. Chernyak, and D. Deka. Ensemble control of cycling energy loads: Markov decision approach. In S. Glavaski I. Hiskens J. Stoustrup S. Meyn, T. Samad, editor, Energy Markets and Responsive Grids: Modeling, Control and Optimization. Springer, Series: Institute of Mathematics and Applications, 2018.
 - [8] C. Y. Chong and A. S. Debs. Statistical synthesis of power system functional load models. In Decision and Control including the Symposium on Adaptive Processes, 1979 18th IEEE Conference on, volume 2, pages 264–269, Dec 1979.
 - [9] C.-Y. Chong and R. P. Malhami. Statistical synthesis of physically based load models with applications to cold load pickup. Power Apparatus and Systems, IEEE Transactions on, PAS-103(7):1621–1628, July 1984.
 - [10] R. P. Feynman. Statistical Mechanics. Advanced Books Classics, Perseus Books, Reading, Massachusetts, 1997.
 - [11] C. W. Gardiner. Handbook of stochastic methods for physics, chemistry and the natural sciences, 3rd ed. Springer Series in Synergetics, vol.13, Berlin: Springer-Verlag, 2004.
 - [12] O. Guéant, J.-M. Lasry, and P.-L. Lions. Mean Field Games and Applications, pages 205–266. Springer Berlin Heidelberg, Berlin, Heidelberg, 2011.
 - [13] M. Huang, R. P. Malhame, and P. E. Caines. Large population stochastic dynamic games: closed-loop McKean-Vlasov systems and the Nash certainty equivalence principle. Commun. Inf. Syst., 6(3):221–252, 2006.
 - [14] S. Ihara and F. C. Schweppe. Physically based modeling of cold load pickup. IEEE Transactions on Power Apparatus and Systems, PAS-100(9):4142–4150, Sept 1981.
 - [15] M. Kamgarpour, C. Ellen, S. E. Z. Soudjani, S. Gerwinn, J. L. Mathieu, N. Müllner, A. Abate, D. S. Callaway, M. Fränzle, and J. Lygeros. Modeling options for demand side participation of thermostatically controlled loads. In 2013 IREP Symposium Bulk Power System Dynamics and Control - IX Optimization, Security and Control of the Emerging Power Grid, pages 1–15, Aug 2013.
 - [16] Y. Kuramoto. Self-entrainment of a population of coupled non-linear oscillators. In International Symposium on Mathematical Problems in Theoretical Physics, pages 420–422. Springer, Berlin, Heidelberg, 1975. DOI:

- 10.1007/BFb0013365.
- [17] Y. Kuramoto. Cooperative Dynamics of Oscillator Community A Study Based on Lattice of Rings. Progress of Theoretical Physics Supplement, 79:223–240, February 1984.
 - [18] L. Landau. On the vibrations of the electronic plasma. Akad. Nauk SSSR. Zhurnal Eksper. Teoret. Fiz., 16:574–586, 1946.
 - [19] J.-M. Lasry and P.-L. Lions. Mean field games. Japanese Journal of Mathematics, 2(1):229–260, Mar 2007.
 - [20] J.E. McDonald and A.M. Bruning. Cold load pickup. PAS-98:1384 – 1386, 08 1979.
 - [21] D. Métivier, I. Luchnikov, and M. Chertkov. Power of Ensemble Diversity and Randomization for Energy Aggregation. arxiv:1808.09555, August 2018.
 - [22] C. Mouhot and C. Villani. On Landau damping. Acta Mathematica, 207(1):29–201, September 2011.
 - [23] M. Nourian and P. Caines. ϵ -nash mean field game theory for nonlinear stochastic dynamical systems with major and minor agents. SIAM Journal on Control and Optimization, 51(4):3302–3331, 2013.
 - [24] D. Paccagnan, M. Kamgarpour, and J. Lygeros. On the range of feasible power trajectories for a population of thermostatically controlled loads. In 2015 54th IEEE Conference on Decision and Control (CDC), pages 5883–5888, Dec 2015.
 - [25] Demand Response. https://en.wikipedia.org/wiki/Demand_response.
 - [26] Steven H. Strogatz. From Kuramoto to Crawford: exploring the onset of synchronization in populations of coupled oscillators. Physica D: Nonlinear Phenomena, 143(1):1–20, September 2000.
 - [27] N. van Kampen. Stochastic Processes in Physics and Chemistry (Third Edition). Amsterdam: Elsevier, 2007.
 - [28] A. A. Vlasov. The Vibrational Properties of an Electron Gas. Soviet Physics Uspekhi, 10(6):721, 1968.